Received Date : 14-Jun-2016

Revised Date : 22-Dec-2016

Accepted Date : 23-Jan-2017

Article type : Standard Paper

Handling Editor: Alison Power

Transmission and temporal dynamics of anther-smut disease *(Microbotryum*) on alpine carnation (*Dianthus pavonius*).

Emily L. Bruns[1*], Janis Antonovics[1], Valentina Carasso[2], and Michael Hood[3]

[1]University of Virginia, Department of Biology, Charlottesville, VA, [2] Ente di gestione delle Aree Protette delle Alpi Marittime, Centro per la Biodiversità Vegetale, Chiusa di Pesio, Italy. [3]Amherst College, Department of Biology, Amherst, MA.

* Corresponding author, elb5m@virginia.edu

SUMMARY

1. Theory has shown that sterilizing diseases with frequency-dependent transmission (characteristics shared by many sexually transmitted diseases) can drive host populations to extinction.
2. Anther-smut disease (caused by *Microbotryum sp.*) has become a model plant pathogen system for studying the dynamics of vector and sexually transmitted diseases: infected individuals are sterilized, producing spores instead of pollen, and the disease is spread between reproductive individuals by insect pollinators. We investigated anther-smut disease

in a heavily infected population of *Dianthus pavonius* (alpine carnation) over an eight-year period to determine disease impacts on host population dynamics.

3. Over the eight years, disease prevalence remained consistently high (>40%) while the host population numbers declined by over 50%.
4. The observed rate of vector transmission to reproductive, adult hosts was inadequate to explain the high disease prevalence. Additional density-dependent aerial transmission to highly susceptible juveniles, indicated from experimental field and greenhouse studies, is likely to play a key role in maintaining the high disease prevalence.
5. Epidemiological models that accounted for the mixed transmission mode predicted an eventual decline in disease.
6. *Synthesis:* Our results demonstrate that high prevalence of a sterilizing disease does not necessarily drive host populations towards extinction and also highlights the importance of demographic studies for establishing the presence of alternative transmission modes.

KEYWORDS: age-specific resistance, demography, epidemiology, frequency-dependent transmission, mixed transmission, plant pathogen, sterilizing disease, vector transmission

INTRODUCTION

With the realization that pathogens form an important component of ecosystem functioning and global change (Hudson, Dobson & Lafferty 2006; Bradley, Gilbert & Martiny 2008) and that they also may play a crucial role in the evolution basic host life history traits (Busch, Neiman & Koslow 2004; Steets *et al.* 2007; Miller & Bruns 2016), there has been an increasing interest in understanding the dynamics of disease in natural plant populations (Alexander 2010; Burdon & Thrall 2014; Tack & Laine 2014). However capturing the demographic and transmission patterns of natural populations is challenging, particularly for longer-lived species, and requires population monitoring over many years. In a recent review, Burdon and Thrall (2014) identified just eight wild plant pathogen systems

where extensive long-term temporal data on disease dynamics have been collected. All of these systems are characterized by metapopulation dynamics; i.e., significant spatial structure in the distribution of host populations and local extinction and colonization dynamics in the pathogen populations. We have very few empirical examples to date where pathogens occur within large continuous wild plant populations (but see Carlsson-Granér, Giles & Thrall 2014).

The impermanence of host-pathogen associations in nature can occur through two proximate mechanisms: local extinction of the pathogen due to the failure of sufficient disease transmission, or pathogen-driven extinction of the host population (and by extension, elimination of the pathogen). Studies of disease within fractured host metapopulations have shown that a transient nature of disease is common, especially in small populations (Smith, Ericson & Burdon 2003; Antonovics 2004; Laine & Hanski 2006; Carlsson-Granér *et al.* 2014). However examples are lacking where pathogens having substantial fitness impacts on the host can stably persist within populations or drive host populations to extinction. Theoretical studies indicate that pathogen-driven host extinction is possible when disease transmission is frequency-dependent, and particularly when infection results in host sterility, rather than mortality (Thrall, Antonovics & Hall 1993a; Boots & Sasaki 2003; Best *et al.* 2011). However, with the exception of emerging diseases that are introduced into naïve populations (Crawford, Lips & Bermingham 2010; Fisher *et al.* 2013), we have very few examples of endemic diseases driving extinction in natural host populations (De Castro & Bolker 2004). More broadly, we still have few empirical measures of the impact of disease on natural plant populations, and the available studies show a wide range of effects (Reviewed in Alexander 2010). For example, Penczykowski *et al.* (2015) found that natural populations of *Plantago lanceolata* infected with powdery mildew had significantly lower population growth rates than uninfected populations. However, Alexander and Mihial (2000) found that a damping off disease that caused high seedling mortality in the legume, *Kummerowia stipulacea* did not translate to declines in host population size.

Here we report the results of a long-term study of anther-smut disease *(Microbotryum*) in a large, heavily infected population of alpine carnations *(Dianthus pavonius*). Our main goals were to determine whether the dynamics within this population were stable or, given the high prevalence of

the sterilizing disease and a presumption of frequency-dependent transmission, would eventually lead to disease-driven host population extinction. We therefore coupled a population census of host and pathogen population size over eight years with year-to-year transition data on individual marked plants and additional experiments to quantify spore deposition and host resistance. We then employed a modelling approach to predict long-term disease dynamics. Our results showed that the high disease prevalence has been facilitated by presence of multiple disease transmission modes. However, our epidemiological model predicts the eventual decline of disease.

METHODS

Study system

Host species

Alpine carnation, *Dianthus pavonius* Tausch (= *D. neglectus* Loisel) is a perennial herbaceous plant endemic to the western Alps in southern France and northern Italy. It is typically found in meadow habitats between 1600m and 2300m in elevation. Flowering occurs for a 2-3 week period in mid summer, but individual plants often do not flower each year. In our study area at ca. 2000m near Rifugio Garelli, in the Parco Naturale del Marguareis, the plant populations form large, more or less continuous stands, often reaching high densities (up to 50 flowering individuals per m^2). Disease prevalence within this local area is exceptionally high (>40%). The average prevalence among diseased populations within the broader Maritime Alps region (ca. 200km^2) is just 13% (Bruns *et al.*, in review).

Pathogen species

Anther-smut disease is caused by a fungal pathogen (*Microbotryum spp.*) that produces spores in the host's anthers in place of pollen. *Microbotryum* infects many hosts in the Caryophyllaceae (Hood *et al.* 2010), but each host species tends to have its own *Microbotryum* species (le Gac *et al.* 2007). Three lineages (putative species) of *Microbotryum* have been found on *D. pavonius* in the

western Alps, but only one has been observed in the populations studied here (Petit et al. *in review*). Moreover, the nearest other diseased *Dianthus* species (*D. furcatus*) is in another valley, 6.5 km away (Bruns *et al. in review*). Disease symptoms in *D. pavonius* are like in other species: infected individuals produce spore-bearing anthers and the ovary fails to mature. The infection is systemic and persistent; usually all flowers are affected resulting in complete sterility of an infected individual.

Anther-smut spores are transported to hosts by insect pollinators. Importantly the infection route is not restricted to the flower but can also occur through the leaves or cotyledons; indeed, placing a spore suspension on a seedling is a standard inoculation protocol (Alexander & Antonovics 1995). The pathogen overwinters inside the host, and the only visible disease symptoms are the production of 'smutty' flowers the following season. This dependency on the host for overwinter survival means that the disease is only maintained on perennial hosts (Thrall, Biere & Antonovics 1993b; Hood *et al.* 2010). Vertical transmission through seed is not possible because infected individuals are sterilized, and has never been observed even in partially diseased plants (Baker 1947). Genetic variation in resistance to anther-smut at the family level is well-documented in *Silene latifolia* (Alexander 1989; Alexander, Antonovics & Kelly 1993) and *S. uniflora* (Chung *et al.* 2012) and appears to be continuous, although the mechanism is unknown.

Empirical studies

Population monitoring

To monitor local disease dynamics, two marked transects were set up near Rifugio Garelli (for details see Supplementary Material, Fig. S1). Transect 1 was established in 2007, spanned 100m in length and varied in width from 5 to 15m. In this study, we focused on temporal dynamics in a 25 x10m section of the transect that contained 88% of the total individuals (Fig. S1) at high density (9.6 individuals per m^2). Transect 2, established in 2009 approximately 0.5km away from Transect 1, was 50m long and varied in width from 1 to 21m. All flowering individuals were counted and scored for disease when the transects were established, and again in 2014 and 2015.

Demography of adult, flowering plants

Marked individuals were followed within the high density section of Transect 1. Individuals were marked using green plastic coated wire around their base, and by a 10-cent US coin placed in the ground ca. 2cm downhill from the plant, so it could be located using a metal detector. Individuals were only included if they were flowering, so that disease status could be determined, and if they were distinct (usually > 10cm) from other individuals; the age of individual plants was not known. A maximum of 2 individuals per 0.5 x 0.5m quadrat were marked to avoid undue disturbance. One set of individuals was marked in 2008 (90 healthy, 22 diseased) and additional individuals were marked in 2009 (118 healthy, 63 diseased) and in 2012 (60 healthy, 40 diseased). Each year we recorded survival, flowering and disease status of marked individuals.

Implant studies with sentinel plants

Healthy adult individuals may have been challenged by disease, and may already have resistance due to age-specific, immunological, or genetic heterogeneities in disease susceptibility. Therefore, we used implant experiments to quantify disease transmission onto individuals that had never been exposed to disease. Individuals from field-collected seeds were raised in a disease-free garden at the base of the mountain (ca. 500m elevation) and then transplanted into the field prior to flowering. In 2013, 1021 one-year old individuals were transplanted at 0.75m spacing into a 12 x 25m rectangular plot within 10m of Transect 2. Individuals were tagged with wire and coins and monitored for survival, flowering, and disease status through 2015. To determine local disease prevalence, in 2014 the naturally occurring plants in the implant plots were censused for disease status.

Spore dispersal

We quantified two routes of spore dispersal; pollinator-vectored dispersal to flowers and passive, aerial dispersal. To estimate spore dispersal to flowers, in 2015 we collected and dried a single recently closed flower from each of 50 healthy individuals in the demography section of Transect 1; each flower came from a different half-meter quadrant. To count spores, collected flowers were cut in half and placed in 1mL of Pohl's solution (25% Methanol, 1.2% Aerosol OT) to soften for

24 hours. *Microbotryum* spores have a reticulate surface (Schäfer *et al.* 2010) and are easily recognizable under the microscope. To facilitate counting, spores were concentrated as follows. Each tube with a flower was vortexed, and a 700µL aliquot centrifuged for 2 minutes to concentrate spores at the bottom. 640μL of supernatant was removed, and the spores in the 60μL concentrate were counted with a hemacytometer at 200X magnification. Two counts for each sample were averaged.

To estimate aerial spore dispersal, sticky spore traps (transparency paper with double-sided adhesive tape) were placed around four large diseased and four large healthy individuals (> 20 inflorescences) that were at least one meter away from other flowering individuals. Spore traps were arranged on three evenly spaced radii (two were 2 x 30cm strips and one was a 2 x 90cm strip) starting at the edge of a plant and orientated at random. After 48h, the traps were covered with a protective sheet of transparency paper and spore counts were made within each 5cm section at 200X magnification.

Age-specific susceptibility

To determine the age-specific susceptibility to anther-smut of *D. pavonius*, we reared plants from field-collected seed (from near Transect 2) at three different times in the University of Virginia greenhouses to obtain three age classes; these were then all inoculated with the same inoculum. Seeds were sterilized (8.25% NaOCl, 20% ethanol for 6 min, rinsed 5 times in sterile water) and nicked with a razor blade to promote germination before planting on agar medium (10% Murashige and Skoog basal medium, 0.75% agar). Ten-day-old seedlings were transplanted to 115cm^2 'Cone-tainers' (Stuewe and Sons, Inc., Corvallis, OR) filled with Promix BX potting soil, and grown with 14h day length of supplemented lights. Approximately 100 seeds were sown in March and January 2013, and April 2014. To provide winter pre-conditions for flowering of the first cohort of plants, they were moved outside from November 2013 to April 2014.

To measure floral resistance, spores from greenhouse-grown diseased plants (infected with *Microbotryum* from near Transect 1) were transferred to a single open flower of the healthy plant using a paintbrush. To inoculate non-flowering plants a 2uL suspension of 500 spores/uL from the

same diseased plant was placed on the apical meristem (seedling cohort) or an axillary meristem (4-month old cohort). Inoculated plants were placed in a dew chamber with 100% relative humidity overnight. Plants were overwintered outside from Nov 2014 to March 2015, and transferred inside for flowering to determine disease status.

Data analysis

Mortality and flowering rates

We used the marked-plant annual data from 2008 to 2015 to calculate year-to-year mortality and flowering rates for flowering-healthy, flowering-diseased, and vegetative individuals; we could not determine the disease status of vegetative individuals. Mortality rates were calculated as the proportion of individuals dying out of those present the year before. Flowering rates were calculated as the proportion of surviving individuals that flowered. To compare mortality and flowering rates among the above flowering states we used mixed generalized linear models with year as a random effect, and a logistic link function.

Pathogen manipulation of life history traits

To determine the effect of anther-smut disease on lifetime inflorescence production, we used 'aster models' that explicitly include the dependence of later life history stages on the expression of earlier life history stages, taking into account differing sampling distributions at each stage (Shaw *et al.* 2008; the 'aster' package in R, Geyer *et al.* 2007). Our model had three life history components each conditioned upon the state in the previous year: (a) survival (b) flowering vs. vegetative, and (c) the number of inflorescences. Bernoulli distributions were used for survival and flowering, and a zero-truncated Poisson distribution for inflorescence number. We used individuals marked in 2009 (the largest group), and excluded the few individuals (n=22) that changed disease status, to avoid confounding effects of infection and recovery.

Infection and recovery rates

Because disease status could only be assessed on flowering plants, and individuals did not flower every year, the infection rate of flowering individuals per year was estimated as the proportion of healthy flowering individuals in any one year that flowered and were diseased in a subsequent year divided by the total number of healthy individuals that flowered again at some point during the study; we term these latter 'scorable' plants. Note that this assumes that only flowering individuals become infected. The force of infection is then the floral infection rate divided by the probability of surviving and flowering. Note that while this calculation assumes that individuals only become infected while flowering it does not specify whether the transmission route was via pollinators or aerial dispersal. The total force of infection on flowering individuals (F_{total}) is then the floral infection rate divided by the probability of surviving and flowering. Recovery rate (γ) was calculated as the total proportion of recovered individuals divided by the proportion of 'scorable' individuals.

In the implant experiment, individuals that were diseased the first time they flowered must have been infected while vegetative, presumably through the aerial transmission route. We calculated the force of infection on vegetative plants due to aerial transmission (F_v) as the fraction of 'scorable' implants that were diseased divided by the probability that an individual survived and flowered during the two-year period. To estimate the density-dependent transmission coefficient, β_v, we divided force of infection by the density of naturally occurring diseased plants in the implant plots.

Modelling Disease Dynamics

The general model

To model the population and disease dynamics we used difference equations because host and pathogen reproduction occurs once a year. Individuals infected in one year do not express disease and are not sterilized until the following year. There were five states: numbers of flowering-healthy (Nfh), flowering-diseased (Nfd), vegetative-healthy (Nvh), vegetative-diseased (Nvd), and juvenile (Nj). The

juvenile stage was defined as individuals that survived to the first year from seed and were not flowering; less than 1% of the 1-year old plants flowered in the greenhouse. We assumed there was no seed bank since five soil samples (10x10x5cm) collected adjacent to the Transect 1 prior to seed set in August 2015, yielded no germinating *D. pavonius* plants (V. Carasso, unpublished data). Only healthy flowering individuals reproduce since infection results in host sterilization. In addition, only flowering diseased plants contribute to the transmission since spores are only produced in the anthers.

The equations are:

$$\mathrm{Nfh}_{t+1} = \mathrm{Nj}_t\phi_j(1-F_j) + \mathrm{Nfh}_t(1-\mu_f)\phi_{fh}(1-F_f)(1-F_v) + \mathrm{Nfd}_t(1-\mu_f)\phi_{fd}\gamma + \mathrm{Nvh}_t(1-\mu_v)\phi_v(1-F_v) + \mathrm{Nvd}_t(1-\mu_v)\phi_v\gamma \quad (1)$$

$$\mathrm{Nfd}_{t+1} = \mathrm{Nj}_t\phi_jF_j + \mathrm{Nfh}_t(1-\mu_f)\phi_{fh}(F_f+F_v) + \mathrm{Nfd}_t(1-\mu_f)\phi_{fd}(1-\gamma) + \mathrm{Nvh}_t(1-\mu_v)\phi_vF_v + \mathrm{Nvd}_t(1-\mu_v)\phi_v(1-\gamma) \quad (2)$$

$$\mathrm{Nvh}_{t+1} = \mathrm{Nj}_t\left(1-\phi_j\right)(1-F_j) + \mathrm{Nfh}_t(1-\mu_f)(1-\phi_f)(1-F_f)(1-F_v) + \mathrm{Nfd}_t(1-\mu_f)(1-\phi_{fd})\gamma + \mathrm{Nvh}_t(1-\mu_v)(1-\phi_v)(1-F_v) + \mathrm{Nvd}_t(1-\mu_v)(1-\phi_v)\gamma \quad (3)$$

$$\mathrm{Nvd}_{t+1} = \mathrm{Nj}_t(1-\phi_j)F_j + \mathrm{Nfh}_t(1-\mu_f)\phi_{fh}(F_f+F_v) + \mathrm{Nfd}_t(1-\mu_f)(1-\phi_{fd})(1-\gamma) + \mathrm{Nvh}_t(1-\mu_v)(1-\phi_v)F_v + \mathrm{Nvd}_t(1-\mu_v)(1-\phi_v)(1-\gamma) \quad (4)$$

$$\mathrm{Nj}_{t+1} = \mathrm{Nfh}_t * b\frac{1}{1+kN} \quad (5)$$

where the state *i* specific rates are: μ_i = mortality, ϕ_i = flowering, Υ_i = recovery, and F_i = the force of infection. Seedling recruitment and survival to the juvenile stage (Eq. 5) was inversely related to density (N). The term *b* describes the production and survival of new seedlings (establishment rate), while *k* describes the strength of density-dependent regulation. Note, that in contrast to models with

discrete, non-overlapping generations, the establishment rate must be considerably higher than the death rate to maintain a stable flowering population size. For reference, in the absence of disease values of *b=1, k=0.00015* lead to a stable population size of 2,500. We assumed that infection did not differentially affect seedling survival, since we have not found any evidence of smut inoculations leading to higher seedling mortality in greenhouse studies (Bruns, *unpublished data*).

We assumed that vector-mediated transmission was frequency-dependent because pollinators are likely to adjust their flight distance in response to plant density (Alexander and Antonovics 1995) but that aerial transmission was density-dependent. The force of infection on flowering individuals through vector transmission was given by:

$$F_f = \beta_f * \frac{\mathrm{Nfd}}{\mathrm{Nfh+Nfd}}$$

(6)while the force of infection on adults and juvenile individuals through aerial transmission was given by:

$$F_v = \beta_v * \mathrm{Nfd}$$

(7)

$$F_j = \beta_v * s * \mathrm{Nfd}$$

(8)

where *s* is a coefficient describing the proportional greater susceptibility of juvenile vs. adult individuals. To avoid negative populations sizes, values were constrained such that $F_i \leq 1$.

The two major empirical unknowns were the transmission mode and the rate of seedling establishment. We tested three assumptions about transmission. The 'pure vector transmission model' assumed that all spore dispersal occurred via insect pollinators and only flowering individuals could become infected (F_v and F_j =0). The 'pure' aerial transmission model' assumed that transmission to

all plant stages (flowering, vegetative, and juvenile) occurred only through density-dependent aerial spore dispersal (F_f =0). The 'mixed transmission model' assumed that that spore dispersal occurred via both pollinator vectors and passive aerial dispersal; flowering individuals could become infected through vectors and aerial dispersal ($F_f + F_v$) while vegetative individuals (including both adult and juvenile stages) could become infected through aerial spore dispersal.

Since it was not possible to get field measurements of the rate of seedling recruitment, we ran simulations with a range of recruitment rates (*b=0.1 to b=2* and *k=0.000075* to *k*=0.001), to calculate the 'best-fit' values of *b* and *k* based on the minimum chi-squared deviance between the predicted and observed numbers of diseased and healthy flowering individuals in 2015.

Parameterizing the model

We used the arithmetic averages from the adult-plant demography study, weighted by sample size each year, for mortality (μ_i), flowering (ϕ_i), recovery (γ) and the total force of infection on adults ($F_f + F_v = F_{total}$). The juvenile flowering rate (ϕ_i) and force of infection on vegetative plants (F_v) were calculated from the implant experiment. We also calculated the weighted geometric mean of each parameter, but the results of the model using these values were not substantially different (see supplementary material).

For the pure vector model, we assumed that all transmission to flowering plants was from frequency-dependent vector transmission and we calculated β_f by dividing F_{total} by the weighted average prevalence in transect one (45%). For the pure aerial model, we assumed that $F_f = 0$, and used the density-dependent aerial transmission rate β_v that was calculated from the implant experiment. In the mixed transmission model, we had to partition the total force of infection on flowering plants estimated in the adult demography study into the frequency-dependent vector component (F_f) and the density-dependent aerial component (F_v). To do this, we determined the contribution of F_v to F_{total} by multiplying β_v by the number of diseased plants in Transect 1. We then

calculated F_f as $F_{total} - F_v$ and divided this number by the weighted average prevalence in Transect 1 to get frequency-dependent vector transmission rate β_f. Since the number of diseased plants in Transect 1 changed over the course of the experiment, this led to a range of estimates for β_f. Simulations run with the maximum and minimum values of β_f did not differ substantially. Further details about the calculation of transmission coefficients, and their effect on model predictions can be found in Appendix A in the supplementary material.

To estimate the relative juvenile susceptibility (*s*), we divided the average infection rate of juveniles in the greenhouse inoculation experiment by the average infection rate of the adult classes.

Population predictions

We used Transect 1 census data from 2007 as the starting population, and compared the predicted results with the observed data from 2014 and 2015. To estimate the number of healthy and diseased vegetative plants in 2007, we multiplied the number of flowering plants by the ratio of the transition rates of $Nf_i \rightarrow Nv_i$ and $Nv_i \rightarrow Nf_i$. For healthy plants this ratio was 2.3, meaning that at any given time there should be approximately twice as many non-flowering individuals as flowering individuals. Within simulations, parameters were selected from random binomial distributions based on the estimated means, and sample size (Table 1). We ran each simulation 100 times and calculated the proportion of simulations in which the predicted disease prevalence fell within the 95% confidence interval of the observed prevalence.

RESULTS

Change in population size and disease prevalence

The number of flowering individuals in Transect 1 declined from 2,415 in 2007 to 1,059 in 2015 (56% decrease; Fig. 1A). Disease prevalence remained high (46.6% in 2007, 44.7% in 2015). These patterns were consistent with data going back to 2005 from a smaller (5x50m) section of

Transect 1 (Fig. 1B). Similar dynamics were observed in Transect 2: population size declined 39% with disease increasing from 33% to 45% (Fig. 1C).

Adult plant demography

Mortality and flowering

The mortality rate of flowering individuals ranged from 5% to 22% across the six years (Table 1, Fig. S2). Individuals that flowered in the previous year had a much higher probability of surviving than vegetative individuals (χ^2= 27.2, df=1, p<0.0001) and were more likely to flower again (χ^2= 58.7, df=1, p<0.0001). Among flowering individuals, disease status did not have a significant effect on survival (χ^2=0.01, p=0.934). Diseased plants tended to have a greater probability of flowering, but the effect was not significant (χ^2=0.95, df=1, p=0.330; Fig. S2). Aster analysis showed that diseased individuals tended to have a higher lifetime inflorescence production (Dev=3.395, p=0.065); inflorescence production over 6 years ranged from 8.5-10.1 (95% CI) for healthy individuals and 9.3-12.0 (95% CI) for infected individuals.

Virulence and recovery

The majority (94%) of diseased individuals were completely sterilized. Recovery rates were rare. Only 5 previously diseased individuals out of 190 'scorable' plants were healthy when they flowered again. Four additional individuals changed status multiple times but these were excluded from the analysis, as they were likely mixed stems of separate diseased and healthy individuals; the overall low rates of infection and recovery make it extremely unlikely that the same plant would go through more than one transition in a six-year period. The weighted average recovery was $\gamma = 0.038$.

Transmission rates

In the implant experiment we were able to determine disease status at first flowering for 173 implants; 2 of these were diseased (95-CI: 0-2%). The probability of a plant surviving and flowering in either the first or second year was 20.1%. The calculated force of infection on vegetative individuals of F_v = 0.055. Based on the density of diseased individuals within the plot (6.48 per m^2), the density-dependent transmission coefficient adjusted for 250m^2 area of Transect 1 was estimated to be $\beta_v = 3.38\text{x}10^{-5}$.

Transmission events in the adult demography experiment were rare: across all 271 marked healthy individuals, only 18 new infections were observed. The total force of infection on adult plants (F_{total}) varied over the seven years of the study with the highest rate occurring in 2012 (Table 1). The weighted average force of infection was $F_{total} = 0.069$.

If we assumed that the force of infection on flowering plants occurred solely through frequency-dependent vector transmission ('pure vector model'), then $\beta_f = 0.153$. If we assumed that the force of infection on flowering plants occurred through both vector and aerial transmission routes ('mixed model'), then β_f ranged from 0.069 to 0.114. Throughout the paper we present results from the mixed model assuming β_f =0.069, because this value provided the best fit to the observed dynamics. The higher value β_f =0.114 generated similar predictions (see supplemental material).

Spore deposition

We observed *Microbotryum* spores on 80% of the healthy flowers sampled. Flowers with spores had an average of 13,600 spores. We found considerable spore deposition on the sticky strips surrounding diseased plants (0 to 14,700 spores per cm^2). Aerial spore deposition was highest within 10cm of diseased plants and declined rapidly with increasing distance (Table 2). The strips surrounding healthy plants had no spores.

Age-specific susceptibility

The seedling stage was most susceptible to infection: 72% of the seedlings (N=44) became infected while only 7% of the adult plants (combined juveniles and adults, N=25) became infected (χ^2= 28.4149, p<0.0001). None of the plants that were florally inoculated became infected (N=15). In the model, we therefore assumed juveniles were ten times as susceptible as adults (s=10).

We also compared our results with 5 previous unpublished inoculation experiments with this host and pathogen species (details in supplementary material). The pattern of low adult susceptibility and high seedling susceptibility was consistent (Fig. 2).

Model predictions

Predicting the observed short-term dynamics

The mixed transmission model with juvenile-specific susceptibility (s=10) provided the best fit to the observed change in the numbers of healthy and diseased individuals (Fig. 3). Within the mixed model, there were several combinations of establishment rate (b) and the density-dependence (k) that provided similar predictions of the observed change in the numbers (Table 3). On average, simulations run with these best-fit values of b and k predicted the flowering population size within 1% of that observed. The lowest estimated rate β_f for the mixed model (0.069) predicted disease prevalence within 4% of that observed (Fig 4B), while the highest estimated rate β_f (0.114) resulted in a slight over prediction of disease (Figure S3 in supplementary material). Aerial transmission accounted for 72-81% of the total transmissions. The pure aerial model had a slightly higher deviance than the mixed model (Table 3), but still predicted disease prevalence with 5% of the observed value (Figure 4C). Juvenile-specific susceptibility was a critical component of both the mixed and pure aerial transmission models: without juvenile-specific susceptibility disease prevalence was under-predicted by 31% and 36% (mixed and pure aerial models, respectively Figure S4).

The pure vector model could not accurately predict the change in numbers of both healthy and diseased individuals (Figure 3). In this model, combinations of *b* and *k* that best explained the dynamics predicted host extinction even in the absence of disease, and under-predicted host population size in the short-term by 15% (Table 3). Combinations of *b* and *k* that accurately predicted the change in population size strongly under-predicted disease prevalence (Figure 4A). Since the demographic studies did not begin until two years after the first full census, exceptionally high transmission rates in those early years (2007 and 2008) may have increased disease. Increasing the floral transmission rate in the first two years to the maximum rate measured at any point in the study (β_f=0.333) improved the fit of the model, but still under-predicted disease (Fig. S5).

Effect of disease on host population decline

To determine the extent to which disease transmission over the eight year period had contributed to the decline in host population size we ran simulations with and without disease transmission (but including extant diseased plants). When the best-fit model was assumed, population size declined 54% even in the absence of additional disease transmission. Continued disease transmission accounted for an additional 2% decline. In identical simulations where the recruitment was higher (enough to maintain an equilibrium population of 2500 in the absence of disease, *b=1, k=0.00015)*, continued disease transmission accounted for an 11% decline in population size.

Long-term predictions

Simulations run with the best-fit mixed transmission model for 150 years into the future predicted a strong drop in population density followed by the loss of the disease (Fig. 5A-B). The same outcome was predicted even if the highest vector transmission rate ($\beta_f = 0.114$) was assumed (Fig. S6).

We ran additional simulations to determine the sensitivity of our long-term predictions to variation in values of *b* and *k*. We found that disease could only be stably maintained if the establishment rate was at least 1.6X higher than our best-fit estimate (e.g. b=0.75, k=0.00015), a value

that over-predicted the population size by 31% in short-term simulations. Predicted equilibrium prevalence at this higher establishment rate was just 3%. Recruitment rates that maintained the population at 2500 (b=1, k=0.00015) predicted a stable equilibrium disease prevalence of 25% (Figure 5C-D). Thus even if the recruitment rate is substantially higher than our best fit estimates, disease is still likely to decline in the long term.

DISCUSSION

Population dynamics

Our main goal was to study the dynamics of a vector-borne, sterilizing disease within a large, heavily diseased host population and to assess its impact on the host population, given that frequency-dependent disease transmission poses high risk for local host extinction (Thrall *et al.* 1993a; Boots & Sasaki 2003; Best *et al.* 2011). While we observed a rapid decline in population size and a high constant level of disease, disease only explained a small portion of this decline. Moreover, neither the observational data on floral disease transmission nor the best fit transmission models incorporating an additional density dependent seedling transmission predicted disease-driven extinction of the host. Instead, our best-fit transmission model predicted an eventual decline of disease prevalence for all reasonable establishment rates. We have less certainty on whether or not disease will persist at all; simulations with the best-fit establishment rates predicted the loss of disease, while simulations with establishment rates that were high enough to maintain population sizes in the absence of disease predicted maintenance of the disease at a lower prevalence. The high prevalence of disease (ca. 44%) in the present day population is therefore likely to be an epidemic peak, rather than a stable equilibrium. An epidemic peak is also consistent with our large-scale spatial survey of disease in the Maritime Alps region that found an average prevalence among diseased populations of just 13% (Bruns *et al. in review*). Typically, disease epidemics in herbaceous plant populations have been observed over the course of a one or a few seasons (Smith *et al.* 2003; Laine & Hanski 2006), but the

long lifespan of both healthy and infected hosts mean that dynamics will occur over a much longer time frame.

Since our earliest, preliminary data only goes back to 2005, we can only speculate about the conditions that led the disease to reach 40% prevalence. Simulations with our best-fit model show that disease is unable to invade a large population (2,500) when introduced at low frequency (0.01%). It is likely that recruitment rates were once higher and have since declined, because the best-fit values of *b* and *k* are too low to explain the current population size. If recruitment rates are set high enough to maintain the current population size (b=1, k=0.00015), the introduction of disease results in an initial 'overshoot' (Fig. S7) in disease prevalence, and this could explain the epidemic peak that the population appears to be in. Declining recruitment rates could be caused by changes in environmental or biotic factors: for example, in our populations we have observed the exit holes of moth larvae (*Hadena* spp.) that eat the developing seeds; however, we have not had the opportunity to quantify this. Another possibility is that heavy spore deposition on flowers limits seed set of healthy plants. Studies of anther-smut on *Silene acaulis* (Marr 1997) and *Gypsophila repens* (López-Villavicencio *et al.* 2005) have found that spore deposition on the stigmas of healthy individuals can reduce seed set even if plants do not become infected. In *D. pavonius*, brushing the stigmas of healthy plants in the greenhouse with a mixture of spores and pollen reduced fruit set by over 90% compared to plants that were only brushed with pollen (Batzel, Bruns et al., unpublished).

Another possibility is that the population was more susceptible to anther smut when the disease was first introduced and has since evolved higher levels of adult resistance. In *Silene latifolia,* experimental studies have shown that the evolution of resistance can lead to substantial declines in transmission rate and a decline in disease over successive years (Thrall and Jarosz 1994, Alexander & Antonovics 1995). In a long-lived host like *D. pavonius,* there could be a substantial delay between the evolution of resistance and the numerical decline in disease.

Transmission mode

An unexpected and important finding from this study was that multiple transmission routes are critical to maintaining the disease. Anther-smut disease has long been held up as a model for studying the dynamics of sexually-transmitted diseases (Lockhart, Thrall & Antonovics 1996; Antonovics 2005) because the transmission occurs between reproductive adults, the effects are sterilizing, and because patterns of spore deposition (Antonovics & Alexander 1992) and disease spread (Biere & Honders 1998; Antonovics 2004) have been better described by frequency- than density-dependent transmission dynamics. However, we have four lines of evidence that aerial-dispersal of spores to susceptible juveniles is playing a critical role in the dynamics. First, we found substantial aerial spore deposition surrounding diseased individuals, through either wind or scatter from pollinator activity. Second, individuals in the implant studies were diseased the first time they flowered, demonstrating transmission to non-flowering plants in the field. Third, juvenile individuals, were ten times more susceptible than adults upon inoculation. Finally, the observed changes in population size and disease prevalence were only predicted by models that included aerial transmission.

The aerial transmission route ('pre-floral infection') has been observed in *Microbotryum* on other host species, including *Silene latifolia* (Alexander & Antonovics 1988; Alexander 1990), *S. dioica* (Carlsson, Elmqvist & Url 1992), *S. rupestris*, and *Lychnis alpina* (Carlsson-Granér 2006). Ryder *et al.* (2007) showed theoretically that the inclusion of a small amount of density-dependent transmission to a disease that is primarily frequency-dependent could increase disease persistence. Similar results have been obtained in models more specific to anther smut in *S. latifolia* (Alexander and Antonovics 1988) and *S. rupestris* (Carlsson-Granér 2006). However, in the latter study 'floral' infections alone were sufficient for disease persistence in *Lychnis alpina*. Interestingly, in the *D. pavonius /* anther-smut system, multiple transmission modes appear to be determined more by host traits than by properties of the pathogen. Our inoculation studies showed that the strong age-specific resistance in *D. pavonius* would limit vector transmission and facilitate aerial transmission. Correspondingly, even though *Microbotryum* spores were present on 80% of sampled flowers, we

observed extremely low rates of flowering-plant infections in the demography study. Differences in the level of disease resistance between juveniles and adults have been observed in many other plant species (Whalen 2005; Develey-Rivière & Galiana 2007). While the mechanism(s) of resistance to anther-smut are not known, our study raises interesting questions about the ways in which selection may operate on age-specific resistance within natural populations. How is it that such high seedling susceptibility is maintained in the face of a completely sterilizing disease? If resistance is physiologically costly and slows development, as has been demonstrated in many systems (Bergelson & Purrington 1996; Susi & Laine 2015) including anther-smut (Biere & Antonovics 1996), selection may favour a later age-of-onset for resistance. Moreover, seedlings are only likely to encounter spores if they germinate in the proximity of a diseased plant, so perhaps strong selection for seedling resistance would only occur in very high density populations. Resistance may also be developmentally constrained, if characters such as waxy cuticle, can only develop later in leaf development.

Fitness effects of disease

Although *Microbotryum* species all cause a similar disease pathology ('smutty' anthers and sterility) on numerous hosts, the fitness consequences can vary dramatically among host species. In this study, anther-smut disease completely sterilized the majority (93%) of infected individuals and recovery was negligible (<4%). These fitness losses are much higher than those reported for anther-smut on *S. latifolia*, where complete sterilization was less common (0-60% of all infections; Buono *et al.* 2014), and over-winter recovery was high (> 60% Biere and Antonovics 1996). Indeed Rausher (1996) calculated that the total loss in lifetime fitness of *S. latifolia* as a result of anther-smut infection approximated the cost of resistance. Like other studies with this disease, we also found that infected plants had more inflorescences; this may be due to fungal manipulation of the host (Alexander & Maltby 1990; Shykoff & Kaltz 1997, 1998) or simply because individuals with more flowers are more likely to become infected (Alexander & Antonovics 1988; Alexander 1989). Differences in plant age may also be a factor since older individuals have had a longer exposure periods are more likely to be infected, and plant size (and floral displays) likely increases with age.

CONCLUSIONS

Our results demonstrate that high levels of a disease, even when it has large fitness effects, does not necessarily presage population extinction, and that interpreting the consequences of disease in natural populations requires multi-year demographic studies, particularly for long-lived organisms. Our study also emphasizes the importance of 'cryptic' transmission routes not immediately evident from expectations based on natural history observations. Although we did not address pathogen variation, this study shows that the presence of alternative transmission routes, and their ecological and evolutionary determinants, may be in large measure also be a property of the host rather than the pathogen, opening up the possibility of important host-pathogen co-evolutionary interactions, not just at the level of infection, but also affecting transmission mode.

ACKNOWLEDGEMENTS

We sincerely thank the staff of the Parco Naturale del Marguareis especially Bruno Gallino, and Ivan Pace for their collaboration, and Adriana and Guido Colombo for their hospitality at Rifugio Garelli. The early data was the result of a travel grant from the University of Sheffield to Mike Boots and Alex Best, and UVA summer assistantships to Jessie Abbate. Additional field assistance was provided by Ben Adams, Colin Antonovics, Audrey Batzel, Amy Blair, Lidia Castagnoli, Dylan Childs, Claudio Ferracciolo, Mary Gibby, Mandy Gibson, Ruth Hamilton, Ed Jones, Marika Mandaglio, Chiara Mattalia, Mike Paetz, Tim Park, Ian Sorrell, and High school students from Liceo Scientifico Tecnologico in Mondovì helped in the field: Arianna Bottero, Maddalena Graci, and Eleonora Ornati. Paco Abiad and Laura Pierce assisted with spore counting. We gratefully acknowledge grant support from the National Science Foundation, DEB-1115899 to JA and DEB-1115765 to MEH, including REU support, and student contributions by Robbie Richards, Anthony Ortiz, Ian Miller, Lisa Rosenthal, Amy Johnson, Noah Lerner, Monroe Wolfe, Molly Scott, Casey Silver, and Sarah Yee,

Adrianna Turner.We also thank two anonymous reviewers for their comments on the manuscript. The authors declare no conflicts of interest.

AUTHOR CONTRIBUTIONS

JA conceived of the initial population and demography study and carried out the earliest population census. EB, JA, VC and MC contributed to the development and execution of the later field studies. EB carried out the greenhouse study, analysed the data, and developed the model. All authors agreed on the final manuscript.

DATA ACCESSABILITY

Data available from the Dryad Digital Repository: http://dx.doi.org/10.5061/dryad.vn707 (Bruns et al. 2017)

REFERENCES

Alexander, H.M. (1989) An experimental field study of anther-smut disease of Silene alba caused by Ustilago violacea: genotypic variation and disease incidence. *Evolution*, **43**, 835–847.

Alexander, H.M. (1990) Epidemiology of anther-smut infection of Silene alba caused by Ustilago violacea: patterns of spore deposition and disease incidence. *Journal of Ecology*, **78**, 166–179.

Alexander, H.M. (2010) Disease in natural plant populations, communities, and ecosystems: insights into ecological and evolutionary processes. *Plant Disease*, **94**, 492–503.

Alexander, H.M. & Antonovics, J. (1988) Disease spread and population dynamics of anther-smut infection of Silene alba caused by the fungus Ustilago violacea. *Journal of Ecology*, **76**, 91–104.

Alexander, H.M. & Antonovics, J. (1995) Spread of anther-smut disease (Ustilago violacea) and character correlations in a genetically variable experimental population of Silene alba. *Journal of Ecology*, **83**, 783–794.

Alexander, H.M., Antonovics, J. & Kelly, A.W. (1993) Genotypic variation in plant disease resistance--physiological resistance in relation to field disease transmission. *Journal of Ecology*, **81**, 325–333.

Alexander, H.M. & Maltby, A. (1990) Anther-Smut Infection of Silene alba Caused by Ustilago violacea : Factors Determining Fungal Reproduction. *Oecologia*, **84**, 249–253.

Alexander, H.M & Mihail, J.D. (2000). Seedling disease in an annual legume: consequences for

seedling mortality, plant size, and popualtion seed production. *Oecologia,* **122,** 346-353.

Antonovics, J. (2004) Long-term study of a plant-pathogen metapopulation. *Ecology, Genetics, and Evolution of Metapopulations* (eds I. Hanski), & O. Gaggiotti), pp. 471–488. Academic Press, Inc.

Antonovics, J. (2005) Plant venereal diseases: insights from a messy metaphor. *The New phytologist*, **165**, 71–80.

Antonovics, J. & Alexander, H.M. (1992) Epidemiology of anther-smut infection of Silene alba (= S . latifolia) caused by Ustilago violacea: patterns of spore deposition in experimental populations. *Proceedings of the Royal Society B-Biological Sciences*, **250**, 157–163.

Baker, H. (1947) Infection of species of Melandrium by Ustilago violacea (Pers.) Fuckel and the transmission of the resultant disease. *Annals of Botany*, **11**, 333–348.

Bergelson, J. & Purrington, C.B. (1996) Surveying patterns in the cost of resistance in plants. *The American Naturalist*, **148**, 536.

Best, A., Webb, S., Antonovics, J. & Boots, M. (2011) Local transmission processes and disease-driven host extinctions. *Theoretical Ecology*, **5**, 211–217.

Biere, A. & Antonovics, J. (1996) Sex-Specific Costs of Resistance to the Fungal Pathogen Ustilago violacea (Microbotryum violaceum) in Silene alba. *Evolution*, **50**, 1098–1110.

Biere, A. & Honders, S. (1998) Anther smut transmission in Silene latifolia and Silene diocia: Impact of host traits, disease frequency, and host density. *International Journal of Plant Sciences*, **159**, 228–235.

Boots, M. & Sasaki, A. (2003) Parasite evolution and extinctions. *Ecology Letters*, **6**, 176–182.

Bradley, D.J., Gilbert, G.S. & Martiny, J.B.H. (2008) Pathogens promote plant diversity through a compensatory response. *Ecology letters*, **11**, 461–9.

Buono, L., López-Villavicencio, M., Shykoff, J. a., Snirc, A. & Giraud, T. (2014) Influence of Multiple Infection and Relatedness on Virulence: Disease Dynamics in an Experimental Plant Population and Its Castrating Parasite (ed BA Vinatzer). *PLoS ONE*, **9**, e98526.

Burdon, J.J. & Thrall, P.H. (2014) What have we learned from studies of wild plant-pathogen associations?-the dynamic interplay of time, space and life-history. *European Journal of Plant Pathology*, **138**, 417–429.

Busch, J., Neiman, M. & Koslow, J.M. (2004) Evidence for maintenance of sex by pathogens in plants. *Evolution*, **58**, 2584–2590.

Carlsson, U., Elmqvist, T. & Url, S. (1992) Epidemiology of anther-smut disease (Microbotryum violaceum) and numeric regulation of populations of Silene dioica. *Oecologia*, **90**, 509–517.

Carlsson-Granér, U. (2006) Disease dynamics, host specificity and pathogen persistence in isolated host populations. *Okios*, **112**, 174–184.

Carlsson-Granér, U., Giles, B.E. & Thrall, P.H. (2014) Patterns of disease and host resistance in spatially structured systems. *European Journal of Plant Pathology*, **138**, 499–511.

Chung, E., Petit, E., Antonovics, J., Pederson, A.B., and Hood, M.E. (2012) Variation in resistance to multiple pathogen species: anther smuts on *Silene uniflora.* **2,** 2304-2314.

De Castro, F. & Bolker, B. (2004) Mechanisms of disease-induced extinction. *Ecology Letters*, **8**,

117–126.

Crawford, A.J., Lips, K.R. & Bermingham, E. (2010) Epidemic disease decimates amphibian abundance, species diversity, and evolutionary history in the highlands of central Panama. *Proceedings of the National Academy of Sciences of the United States of America*, **107**, 13777–82.

Develey-Rivière, M.P. & Galiana, E. (2007) Resistance to pathogens and host developmental stage: A multifaceted relationship within the plant kingdom. *New Phytologist*, **175**, 405–416.

Fisher, M.C., Henk, D.A., Briggs, C.J., Brownstein, J.S., Madoff, L.C., McCraw, S.L. & Gurr, S.J. (2013) Emerging fungal threats to animal, plant and ecosystem health. *Nature*, **484**, 1–18.

le Gac, M., Hood, M.E., Fournier, E. & Giraud, T. (2007) Phylogenetic evidence of host-specific cryptic species in the anther smut fungus. *Evolution*, **61**, 15–26.

Geyer, C.J., Wagenius, S. & Shaw, R.G. (2007) Aster models for life history analysis. *Biometrika*, **94**, 415–426.

Hood, M.E., Mena-Alí, J.I., Gibson, A.K., Oxelman, B., Giraud, T., Yockteng, R., Arroyo, M.T.K., Conti, F., Pedersen, A.B., Gladieux, P. & Antonovics, J. (2010) Distribution of the anther-smut pathogen Microbotryum on species of the Caryophyllaceae. *The New phytologist*, **187**, 217–29.

Hudson, P.J., Dobson, A.P. & Lafferty, K.D. (2006) Is a healthy ecosystem one that is rich in parasites? *Trends in Ecology and Evolution*, **21**, 381–385.

Laine, A.L. & Hanski, I. (2006) Large-scale spatial dynamics of a specialist plant pathogen in a fragmented landscape. *Journal of Ecology*, **94**, 217–226.

Lockhart, A.B., Thrall, P.H. & Antonovics, J. (1996) Sexually transmitted diseases in animals: ecological and evolutionary implications. *Biological Review*, **71**, 415–471.

López-villavicencio, A.M., Branca, A., Giraud, T., Shykoff, J.A., American, S., May, N. & Lopez-villavicencio, M. (2005) Sex-specific effect of Microbotryum (Uredinales) spores on healthy plants of the gynodioecious Gypsophila repens (Caryophyllaceae). *American Journal of Botany*, **92**, 896–900.

Marr, D.L. (1997) Impact of a pollinator-transmitted disease on reproduction in healthy Silene acaulis. *Ecology*, **78**, 1471.

Miller, I. & Bruns, E.L. (2016) The effect of disease on the evolution of females and the genetic basis of sex in populations with cytoplasmic male sterility. *Proceedings of the Royal Society B-Biological Sciences*, **283**.

Penczykowski, R.M., Walker, E., Soubeyrand, S., & Laine, A-L. (2015). Linking winter conditions to regional disease dynamics ina a wild plant-pathogen metapopualiton. *New Phytologist*, **205,** 1142-1152.

Rausher, M.D. (1996) Genetic Analysis of coevolution between plants and their natural enemies. *Trends in Genetics*, **12**, 212–217.

Ryder, J.J., Miller, M.R., White, A., Knell, R.J. & Boots, M. (2007) Host-parasite population dynamics under combined frequency- and density-dependent transmission. *Oikos*, **116**, 2017–2026.

Schäfer, A.M., Kemler, M., Bauer, R. & Begerow, D. (2010) The illustrated life cycle of Microbotryum on the host plant Silene latifolia. *Botany*, **88**, 875–885.

Shaw, R.G., Geyer, C.J., Wagenius, S., Hangelbroek, H.H. & Etterson, J.R. (2008) Unifying life-history analyses for inference of fitness and population growth. *American Naturalist*, **172**, E35–E47 ST – Unifying life–history analyses for i.

Shykoff, J.A. & Kaltz, O. (1997) Effects of the anther smut fungus Microbotryum violaceum on host life-history patterns in Silene latifolia (Caryophyllaceae). *International Journal of Plant Sciences*, **158**, 164–171.

Shykoff, J.A. & Kaltz, O. (1998) Phenotypic changes in host plants diseased by Microbotryum violaceum: Parasite manipulaiton, side effects, and trade-offs. *International Journal of Plant Sciences*, **159**, 236–243.

Smith, D.L., Ericson, L. & Burdon, J.J. (2003) Epidemiological patterns at multiple spatial scales: An 11-year study of a Triphragmium ulmariae-Filipendula ulmaria metapopulation. *Journal of Ecology*, **91**, 890–903.

Steets, J.A., Wolf, D.E., Auld, J.R., Ashman, T. & Steets, A. (2007) The role of natural enemies in the expression and evolution of mixed mating in hermpahroditic plants and animals. *Evolution*, **61**, 2043–2055.

Susi, H. & Laine, A.-L. (2015) The effectiveness and costs of pathogen resistance strategies in a perennial plant. *Journal of Ecology*, **103**, 303–315.

Tack, A.J.M. & Laine, A.L. (2014) Spatial eco-evolutionary feedback in plant-pathogen interactions. *European Journal of Plant Pathology*, **138**, 667–677.

Thrall, P.H., Antonovics, J. & Hall, D.W. (1993a) Host and pathogen coexistence in sexually transmitted and vector-borne diseases characterized by frequency-dependent disease transmission. *The American Naturalist*, **142**, 543–552.

Thrall, P.H., Biere, A. & Antonovics, J. (1993b) Plant life-history and disease susceptibility- the occurrence of Ustilago violacea on different species within the Caryophyllaceae. *Journal of Ecology*, **81**, 489–498.

Thrall, P.H. & Jarosz, A.M. (1994) Host-pathogen dynamics in experimental populations of Silene alba and Ustilago violacea . II . Experimental tests of theoretical models. *Journal of Ecology*, **82**, 561–570.

Whalen, M.C. (2005) Host defence in a developmental context. *Molecular Plant Pathology*, **6**, 347–360.

Bruns et al. (2017). Data from: Transmission and temporal dynamics of anther-smut disease (Microbotryum) on alpine carnation (Dianthus pavonius).. Dryad Digital Repository. doi:10.5061/dryad.vn707

Table 1. Mortality, flowering, recovery, and force of infection parameters calculated from adult demography study

Year	μ_f	μ_v	ϕ_{fh}	ϕ_{fd}	ϕ_v	γ	F_{total}	N(μ_f)[1]	N(μ_v)	N(ϕ_{fh})	N(ϕ_{fd})	N(ϕ_v)	N(β_f)
2009	0.054	0.258	0.620	0.818	0.356	0.052	0.054	111	83	83	*22*	61	70
2010	0.074	0.174	0.833	0.708	0.796	0.030	0.076	243	46	152	73	38	124
2011	0.143	0.274	0.484	0.464	0.286	0.119	0.070	136	73	109	47	53	74
2012	0.226	0.291	0.640	0.900	0.392	0.000	0.000	84	127	45	20	90	29
2013	0.170	0.307	0.718	0.779	0.260	0.050	0.143	153	88	83	44	61	60
2014	0.093	0.298	0.578	0.786	0.561	0.000	0.000	86	94	46	32	66	32
2015	0.070	0.118	0.565	0.615	0.340	0.000	0.000	71	68	39	27	60	20
Mean[2]	**0.116**	**0.258**	**0.664**	**0.704**	**0.356**	**0.038**	**0.069**						

[1] Sample size used to calculate parameters

[2] Weighted by sample size.

Additional parameters used in the simulations were: ϕ_j = 0.17, [5], *s=10.*

Table 2. Average number of spores found on sticky traps at increasing distance away from a central diseased plant.

Distance (cm)	N	Mean	Sd
0-5	12	1134	2483
5-10	12	287	469
10-25	36	96	243
25-50	24	48	100
50-90	24	36	124

Table 3. Best fit establishment rates for three different transmission models.

Model	*k*	Best-fit b	Equil. Pop. Size[1]	Percent difference from observed Nf[2]	Prevalence[3]	Total Deviance[4]
Pure-vector	0.000075	0.275	0	-13.6%	-25.4%	60.40
$\beta_f = 0.153$	0.00015	0.325	0	-14.6%	-24.6%	60.20
$\beta_v = 0$	0.0003	0.425	10	-15.5%	-24.0%	60.47
	0.0006	0.65	340	-14.9%	-24.6%	60.78
	0.001	0.925	480	-15.3%	-24.3%	60.94
Mixed	0.000075	0.375	0	-2.3%	-4.1%	1.94
$\beta_f = 0.069$	0.00015	0.475	225	<1%	4.9%	1.96
$\beta_v = 3.38\text{x}10 - 5.$	0.0003	0.65	680	<1%	-5.4%	2.48
	0.0006	0.975	875	<1%	-5.9%	2.91
	0.001	1.4	950	-1.1%	-6.1%	3.20
Pure Aerial	0.000075	0.35	0	-7.9%	-5.0%	15.32
$\beta_f = 0$	0.00015	0.4	0	-7.9%	-5.0%	16.20
$\beta_v = 3.38\text{x}10 - 5.$	0.0003	0.55	350	-7.9%	-5.0%	17.06
	0.0006	0.825	630	-7.9%	-4.8%	18.16
	0.001	1.2	750	-7.9%	-5.0%	18.85

[1] Average equilibrium population size in the absence of disease.

[2] Proportional difference between the predicted and observed population size in 2015. (obs.-pred.)/obs.

[3] Proportional difference between the predicted and observed disease prevalence.

[4] Total Chi^2 deviance between the predicted and observed numbers of healthy and diseased individuals.

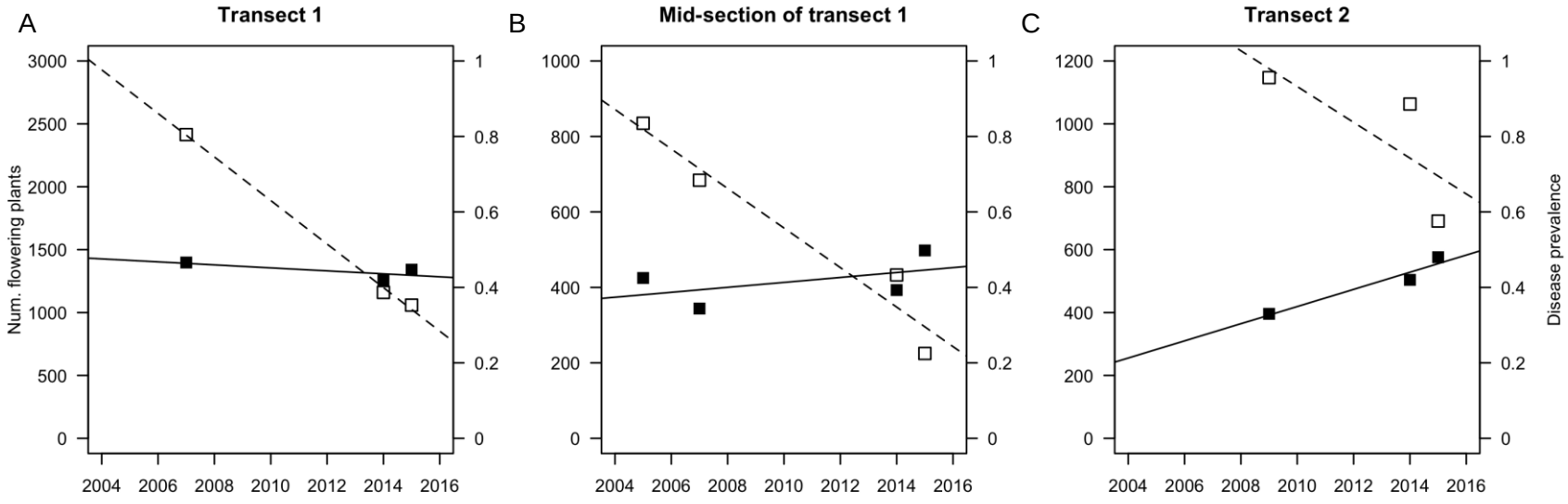

Figure 1. Change in the number of flowering individuals (open boxes, left axis) and disease prevalence (filled boxes, right axis) for A) The high density section of Transect 1, with the first census in 2007, B) A 5x50m subset of Transect 1 where we have census data starting in 2005, and C) Transect 2 with the first census in 2009. *Dashed lines*: best-fit line to total flowering individuals. *Solid lines:* best-fit line to disease prevalence.

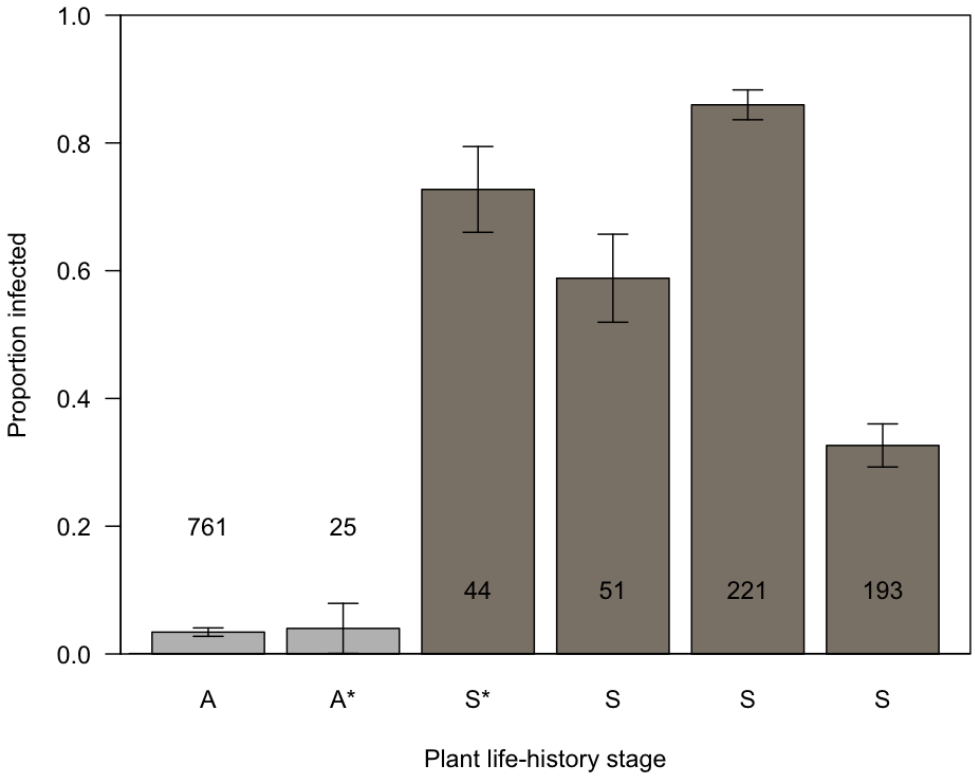

Figure 2. Results of five different greenhouse inoculation experiments conducted on either adult plants (light bars) or seedlings (dark bars). Asterisks indicate the results from the experiment carried out for this study. Numbers indicate sample size, error bars are ± 1 SE. All experiments used seeds and inoculum originating near the main study site. All previous experiments were carried out by placing 2uL of a 500spores/*u*L suspension near the apical meristem. Additional details are in supplementary material.

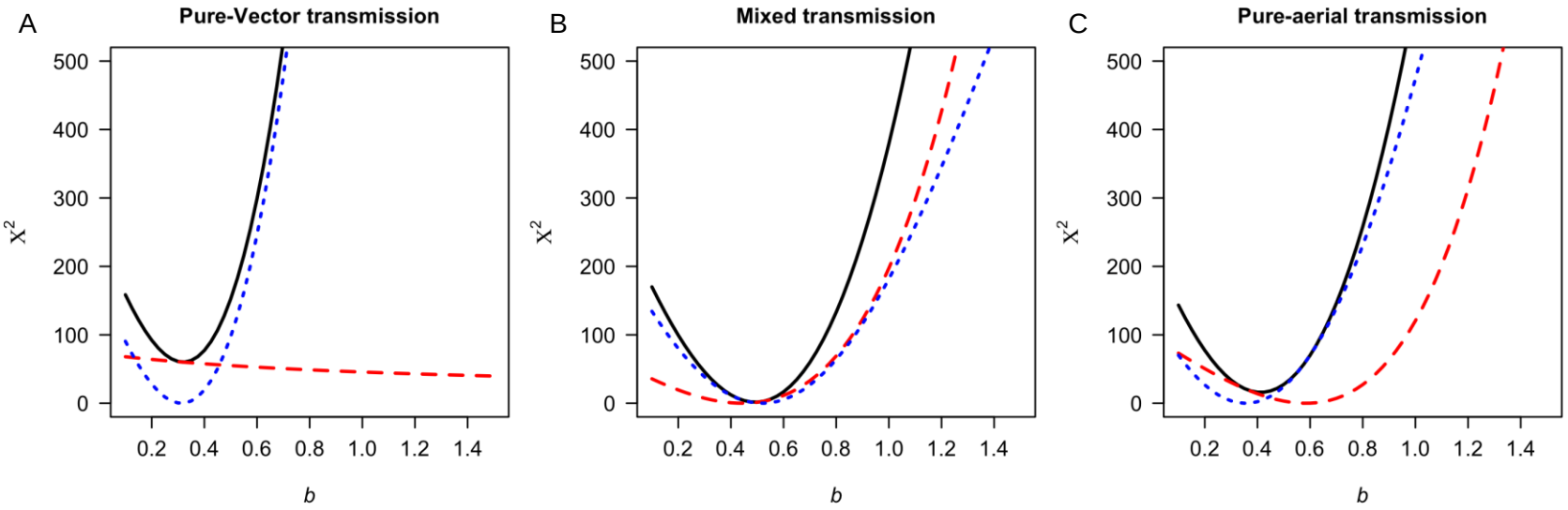

Figure 3. The effect of establishment rate on the ability of three different transmission models to accurately predict the observed short-term dynamics. Model fit is shown as chi-squared deviance from the observed value in 2015, with lower levels of deviance indicating better-fit models. *Blue dashed lines:* number of healthy flowering individuals, *Red dashed lines:* number of diseased flowering individuals, *Solid black lines:* total deviance. The best-fit establishment rate for each transmission model is the value of b that minimizes the total chi-squared deviance. For all simulations: $k=0.00015$. In the mixed model, $\beta_f = 0.069$.

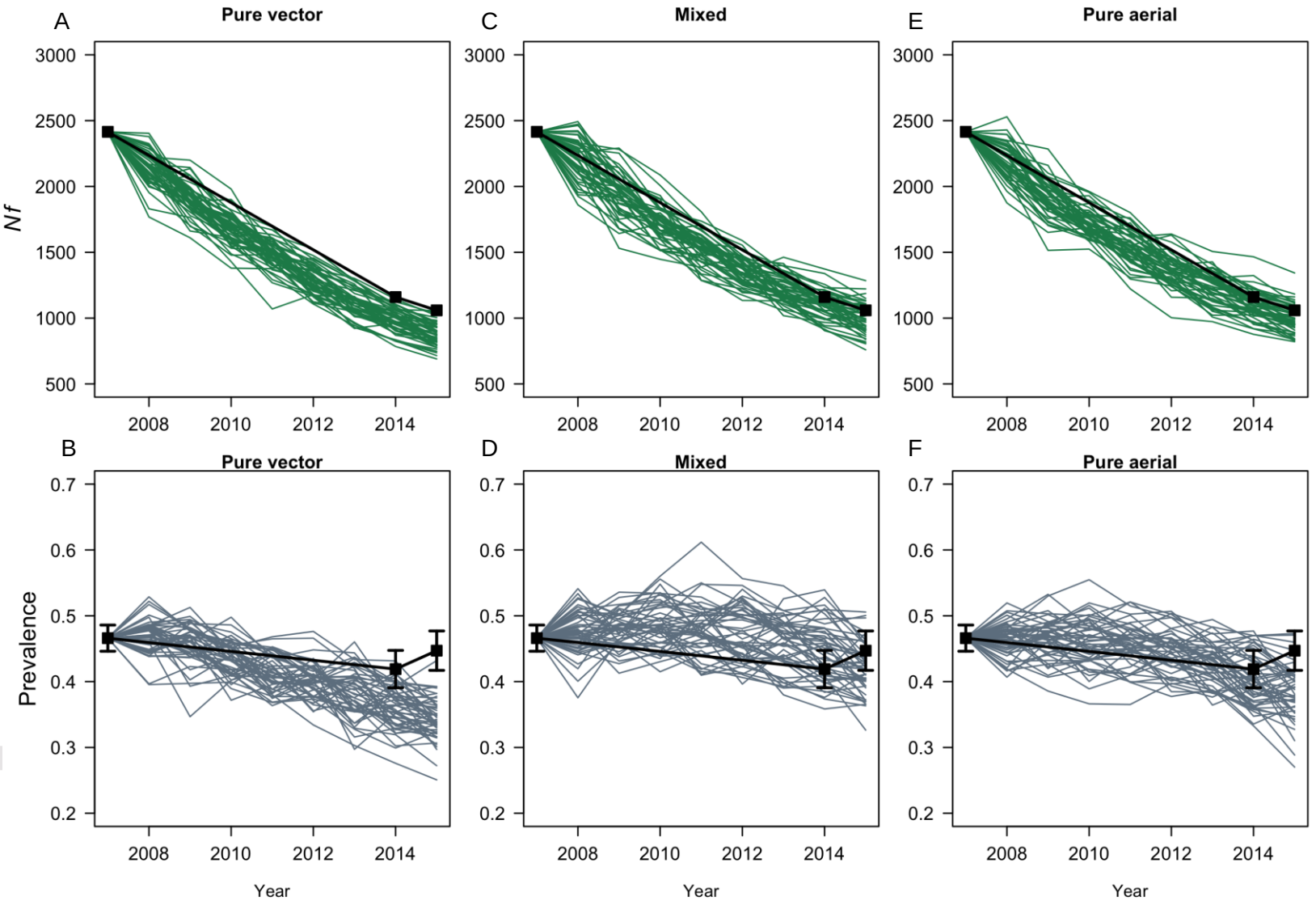

Figure 4. Predicted short-term dynamics for three different transmission models, assuming best-fit establishment rates. Top row shows predicted population size, bottom row shows predicted disease prevalence. *Green and Grey lines:* predicted outcomes from simulations. *Solid black lines:* observed dynamics. A-B) Pure vector transmission ($\beta_f = 0.153, \beta_v = 0, b = 0.325$). C-D) Mixed transmission ($\beta_f = 0.069, \beta_v = 3.38\text{x}10^{-5}, b = 0.475$). E-F) Pure aerial transmission ($\beta_f = 0,\ \beta_v = 3.38\text{x}10^{-5}, b = 0.4$). For all simulations *k=0.00015*.

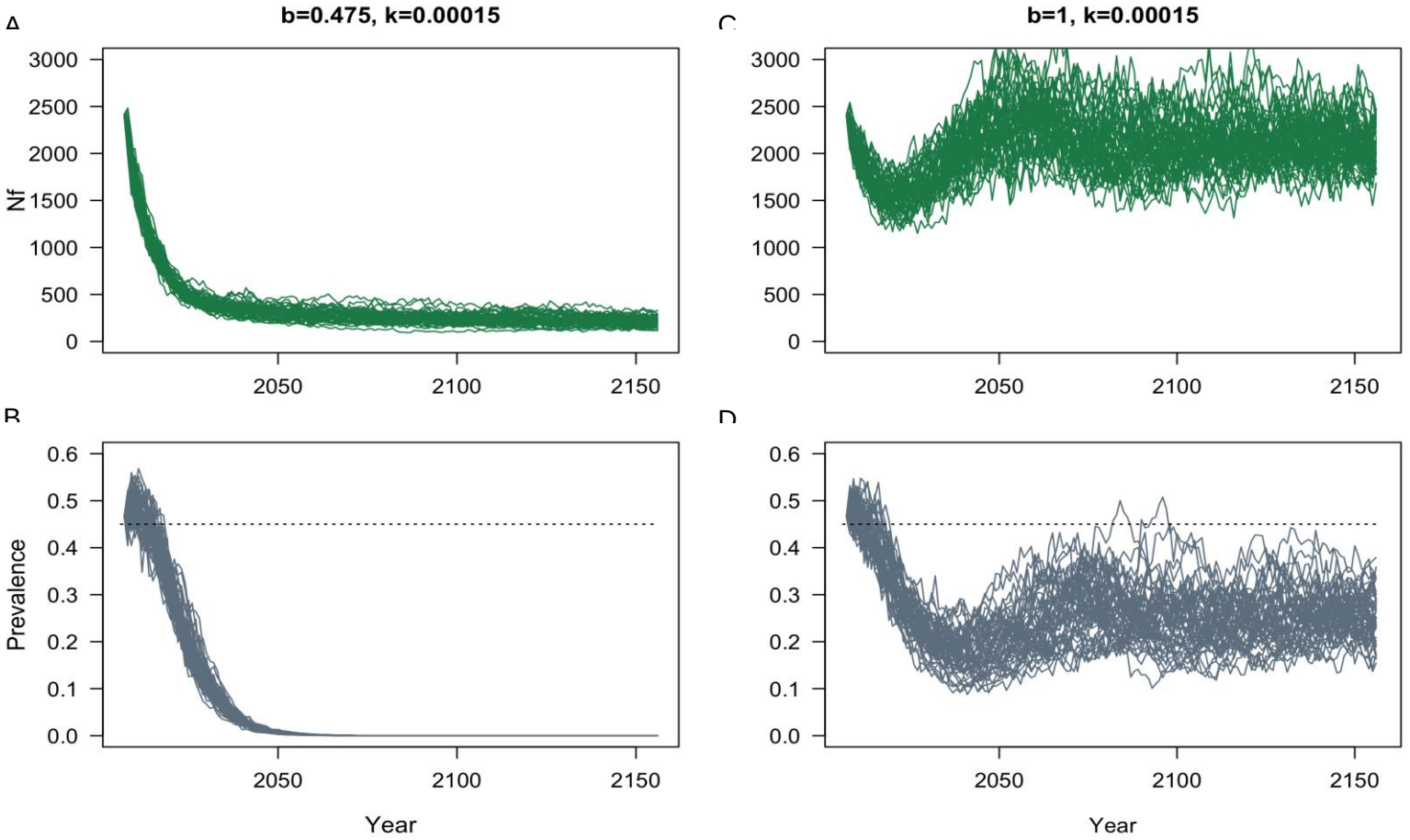

Figure 5. Predicted long-term dynamics under the mixed-transmission model for two different establishment rates. A-B) best fit rates b=0.5, C-D) replacement rates; b=1. The dashed grey line indicates the current disease prevalence. For all simulations $\beta_f = 0.069, \beta_v = 3.38\text{x}10^{-5}, \text{k} = 0.00015$.